Low Cost Implementation of a Wind Turbine Emulator

Liviu – Dănuț Dănuț
Department of Electrical Engineering
Politehnica University of Timisoara
Timisoara, Romania
danut.vitan@upt.ro

Dan Hulea
Department of Electrical Engineering
Politehnica University of Timisoara
Timisoara, Romania
dan.hulea@upt.ro

Octavian Cornea
Department of Electrical Engineering
Politehnica University of Timisoara
Timisoara, Romania
octavian.cornea@upt.ro

Nicolae Muntean
Department of Electrical Engineering
Politehnica University of Timisoara
Romanian Academy-Timisoara Branch
Timisoara, Romania
nicolae.muntean@upt.ro

Mihai Andrei Iuoras
Departament of Electrical Machines and Drives
Technical University of Cluj-Napoca
Cluj-Napoca, Romania
adrian.iuoras@emd.utcluj.ro

Nikolay Hinov
Department of Power Electronics
Technical University of Sofia
Sofia, Bulgaria
hinov@tu-sofia.bg

***Abstract*—This paper presents a low-cost implementation of a hardware-in-the-loop wind turbine emulator (WTE). An induction motor driven by a frequency converter, controlled with a low-cost industrial device, were used to emulate the wind turbine. The controller implements the dynamic equations of the wind turbine, as a function of the wind speed. The induction motor is mechanically coupled with a synchronous generator (the real part of the emulator) designed for a wind energy conversion system. Experimental and simulation results are presented for validation.**

Keywords—wind turbine emulator, intelligent relay, low-cost, hardware-in-the-loop, PMSG

I. Introduction

In recent years an increase in the popularity of microgrids has occurred, together with an intensive development in energy generation, storage and control technologies. Energy generation is an important part in microgrids, and together with the photovoltaic energy, the wind energy is a staple renewable resource having advantages in terms of cost, efficiency and environmental impact [1]–[4].

In the early stages of development for the wind turbine elements, laboratory tests are needed to have reproducible results under different conditions, and a "hardware-in-the-loop" wind turbine emulator (WTE) is well suited for this purpose. Tests can be performed for the generator, the power converters, power extraction algorithms, or even their influence in a microgrid, with the help of a WTE.

Two different classifications of WTEs can be considered, either by the motor type, or by the control implementation platform. Most WTEs make use of costly simulation/programming environments such as Matlab-Simulink or Labview with hardware platforms such as dSpace [5]–[8], OPAL-RT [9], CompactRIO [10], DAQ interfaces [11]–[13], FPGA [14] or DSP [15]–[18] control boards with PC interface. A more industrial approach is also implemented in [19], having the wind turbine model integrated directly in the frequency converter through its SoftPLC function. As with these implementation methods for the WTE, a compromise is made between cost, performance and reliability.

This paper proposes an emulator configuration for implementing the turbine system model by using industrial equipment, with the main control implemented in an intelligent relay, having the advantage of low-cost implementation, together with simplicity, high reliability, ease of use, and high integrability to other systems, such as SCADA.

Supported by the Romanian Ministry of Research and Innovation.

II. WTE Structure

The block diagram of the WTE is shown in Fig.1. It consists of a three-phase squirrel cage induction motor (IM) driven by a frequency converter which is fed from the grid. The frequency converter has the capability to control the speed or the torque through high-performance vector control (direct torque control – DTC). The shaft speed and torque are estimated with good accuracy and the data are sent to the intelligent relay (the core of the system), using ethernet network. The WT mathematical model is implemented using programming blocks. The intelligent relay sends the reference speed back to the frequency converter, computed from the WTE mathematical model and the reference wind speed, obtained via an ethernet network or internally from the relay, using the functional keys.

The IM is coupled through a gearbox (GB) with a permanent magnet synchronous generator (PMSG) – the real part of the emulator, designed for a wind energy conversion system. The GB is necessary because the IM has a higher nominal speed than PMSG. The electrical power provided by the PMSG is injected into the grid using a diode bridge rectifier (DB) and a single-phase inverter.

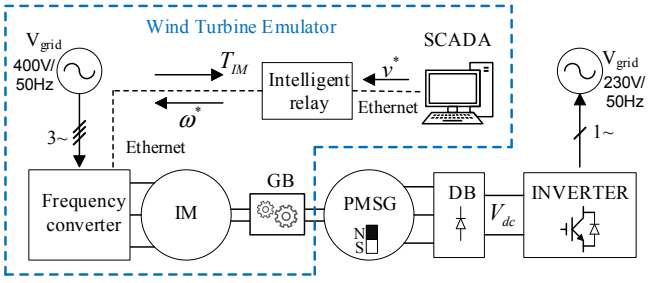

Fig. 1. WTE block diagram

A. Wind Turbine Model

Modeling the rotor blade of a wind turbine is based on the conversion of the available power, correlated with the speed of the wind, into mechanical power. The equation that gives the available wind power in the area swept by the wind turbine blades is [20]:

978-1-7281-7455-6/20/$31.00 ©2020 IEEE

$$P_w = \frac{1}{2} \cdot \rho \cdot A \cdot v^3 \quad (1)$$

where ρ is the specific air density, in [kg/m^3]; A is the blade swept area, in [m^2] and v is the wind speed, in [m/s].

Equation (1) is obtained from the time derivative of the wind kinetic energy considering the wind speed v to be constant:

$$P_w = \frac{dE_k}{dt} = \frac{1}{2} \cdot \frac{dm}{dt} \cdot v^2 \quad (2)$$

$$E_k = \frac{1}{2} \cdot m \cdot v^2 \quad (3)$$

$$m = \rho \cdot A \cdot d \cdot t \quad (4)$$

where m is the air mass, d is the distance and t is the time.

From the total wind power, only a part can be transmitted to the wind turbine shaft. In this case, the mechanical power that can be converted into electrical power is given by the following equation:

$$P_{\text{wt}} = C_P(\lambda, \beta) \cdot P_{\text{w}} = \frac{1}{2} \cdot C_P(\lambda, \beta) \cdot \rho \cdot A \cdot v^3 \quad (5)$$

In (5) the power coefficient of the wind turbine, $C_P(\lambda, \beta)$ is a function of the tip-speed ratio λ and blade pitch angle β. It has a maximum theoretical value of 0.59 which is known as Betz limit and represents the maxim efficiency for a wind turbine. For low power wind turbines, usually, β is constant, therefore the dependence on β is not taken into consideration in this paper. At each moment, λ can be calculated by (6):

$$\lambda = R \cdot \frac{\omega}{v} \quad (6)$$

where R is the radius of the circle traced by the turbine blades and ω is the shaft speed.

The power coefficient is related to the torque coefficient of the wind turbine, $C_T(\lambda)$, through the following equation:

$$C_P(\lambda) = \lambda \cdot C_T(\lambda) \quad (7)$$

$C_T(\lambda)$ must be determined for each wind turbine design. It can be obtained through advanced theoretical and digital simulation techniques. For the wind turbine presented in this paper, the torque coefficient is calculated by (8).

$$C_{\text{T}}(\lambda) = C_{\text{T0}} + a \cdot \lambda - b \cdot \lambda^{2.5} \quad (8)$$

The values of the constant coefficients C_{T0}, a and b are listed in TABLE I. , Section III. Replacing $C_T(\lambda)$ with the right part of (8), equation (7) becomes:

$$C_{\text{P}}(\lambda) = C_{\text{T0}} \cdot \lambda + a \cdot \lambda^2 - b \cdot \lambda^{3.5} \quad (9)$$

The following equations, that express the relation between wind turbine torque, T_{wt}, and $C_P(\lambda)$, $C_T(\lambda)$, can be obtained from (5) to (7):

$$T_{\text{wt}} = \frac{P_{\text{wt}}}{\omega} = \frac{1}{2 \cdot \omega} \cdot \rho \cdot A \cdot C_P(\lambda) \cdot v^3 \quad (10)$$

$$T_{\text{wt}} = \frac{1}{2} \cdot \rho \cdot A \cdot R \cdot C_T(\lambda) \cdot v^2 \quad (11)$$

B. Electrical Model

The electrical model includes the equation which characterizes the PMSG, DB and the inverter. This model is necessary in order to simulate the entire system because for the real implementation, all three parts exist.

In steady state, the equations which covers the electrical model can be written as follow [20]:

$$p_p \cdot \omega \cdot \sqrt{\psi_{PM}^2 - \left(L_s \cdot I_{fp}\right)^2} - \left[R_s \cdot I_{fp} + \frac{6}{\pi} \cdot \left(\frac{V_{DC}}{2} + V_{DB} \right) \right] = 0 \quad (12)$$

$$V_{DC} = \frac{1}{C_f} \cdot \int \left(I_{DC} - I_{load} \right) \cdot dt, \quad (13)$$

$$I_{DC} = \frac{2}{\pi} \cdot I_{fp}, \quad (14)$$

where p_p is the PMSG pole pairs number; ω is the angular speed, in [rad/s]; ψ_{PM} is the linkage flux given by permanent magnet, in [Wb]; L_s is the synchronous inductance, in [H]; I_{fp} is the peak phase current, in [A]; R_s is the stator resistance; V_{DC} is the rectified voltage, in [V]; C_{f} is the DB filter capacitance, in [F]; I_{load} is the load current given by the coupled load in the PMSG stator and V_{DB} is the voltage drop across the diode bridge rectifier in [V].

In order to obtain the angular speed of the wind turbine, the torque of the PMSG is necessary and is described by the next equation:

$$T_g = 1.5 \cdot p_p \cdot \omega \cdot \sqrt{\psi^2{}_{PM} - \left(L_s \cdot I_{fp}\right)^2} + \omega \cdot k_{pFe} \quad (15)$$

The core losses depends of the angular speed and are considered in equation (15) through k_{pFe} which is core loss coefficient.

C. Mechanical Model .

The angular speed of the wind turbine and of the PMSG is determined using the dynamic equation of motion:

$$T_{wt} - T_g = J \cdot \frac{d\omega}{dt} \quad (16)$$

where J represent the total inertia of the wind turbine system and is the sum between wind turbine and PMSG inertia. Their values are given in TABLE I. and TABLE II. :

$$J = J_{wt} + J_g \quad (17)$$

III. WTE IMPLEMENTATION

WTE Implementation is based on an existing five blades, fixed-pitch, wind turbine, Fig. 12. Based on the mathematical model and on the parameters of the wind turbine from TABLE I. the power coefficient (C_{P}) versus tip – speed ratio (λ) is presented in Fig. 2. It can be observed that the C_{P} has a maximum value which is given at an optimal TSR.

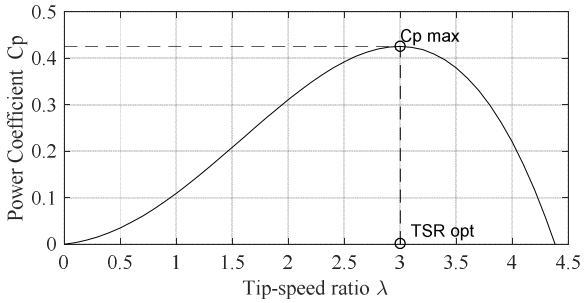

Fig. 2. Power coefficient (C_P) versus Tip – speed ratio (λ)

The wind turbine characteristics, power and torque versus angular speed are presented in Fig. 3, for the wind speed values between 0.5 and 10 m/s. Among the characteristics is shown the load curve implemented in the inverter. The load curve depends on the DC voltage but being a PMSG the DC voltage is dependent to the angular speed.

In general, the intelligent relays have limitations regarding processing capabilities, usually been used in simple residential applications where handling with advanced computation is not needed.

The intelligent relay used in this application operates with 16-bit integers and does not have root and power functions. In addition, because of the very low value of the wind turbine coefficients is very difficult and impractical to work with them.

From the dynamic equation, it can be observed that the only important parameter from the mathematical wind turbine model is the wind turbine torque T_{wt}. In order to be implemented in the intelligent relay, the wind turbine torque characteristics were approximated with eleven third-degree polynomials. The third-degree polynomial is a good compromise between precision and the computational requirements. The coefficients for the eleven polynomials are provided in TABLE III.

Fig. 4 shows a comparison between a theoretical characteristic and a polynomial approximation, for v = 9 m/s. A small deviation from the theoretical characteristic is present at low speed, which can be neglected because the

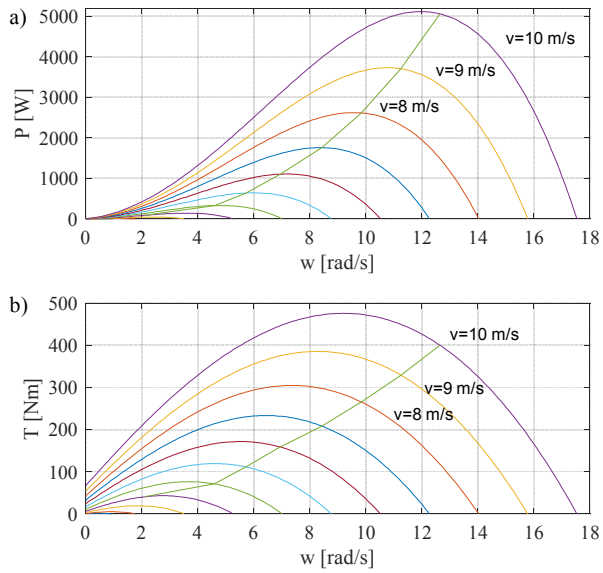

Fig. 3. Wind turbine characteristics a) Power vs angular speed; b) Torque vs angular speed

loading curve of the inverter does not have a steady state operation point in that position.

A linear interpolation is performed between each two adjacent characteristics using:

$$y_2 = \frac{(x_2 - x_1)\cdot(y_3 - y_1)}{x_3 - x_1} + y_1 \tag{18}$$

where: x_1, y_1 are the wind speed and torque of the first characteristic; x_2, y_2 are the actual wind speed and calculated torque; x_3, y_3 are the wind speed and torque of the second characteristic. The number of characteristics was chosen by multiple trials, from which it was found that the linear interpolation has a very good precision for the minimum number of eleven characteristics.

The architecture of the implemented software in the intelligent relay is shown in Fig. 5. The actual torque is acquired as a percentage of the nominal torque of the IM, from the frequency converter. The PMSG torque, T_g, is calculated from the IM torque considering the inertia of the hardware system and the GB, which must be compensated. The total inertia of the hardware system is:

$$J_{hd} = J_{IM} + J_{GB} + J_g \tag{19}$$

$$J_{GB} = J_{IM}\cdot\left(n_{GB}^2 - 1\right) \tag{20}$$

where J_{hd} is the inertia of the hardware system, J_{GB} is the inertia of the GB and the n_{GB} is the GB gearbox coefficient.

The compensation torque is calculated using the dynamic equation (21) by taking into consideration inertia of the IM and the GB.

$$T_c = n_{GB}^2 \cdot J_{IM} \cdot \frac{d\omega}{dt} \tag{21}$$

The speed derivative necessary for calculation of compensation torque is obtained from (16) and then the PMSG torque is calculated using (22).

$$T_g = T_{IM} - n_{GB}^2 \cdot J_{IM} \cdot \frac{d\omega}{dt} \tag{22}$$

The wind turbine torque is calculated based on the eleven polynomials and the interpolation equation (18). The actual speed of the IM, estimated by the frequency converter, is forwarded to all polynomials.

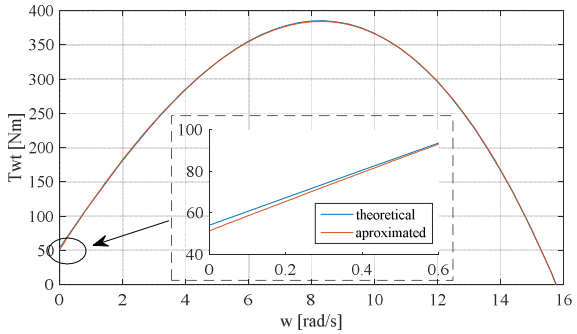

Fig. 4. Theoretical wind turbine torque versus aproximated torque, v = 9m/s

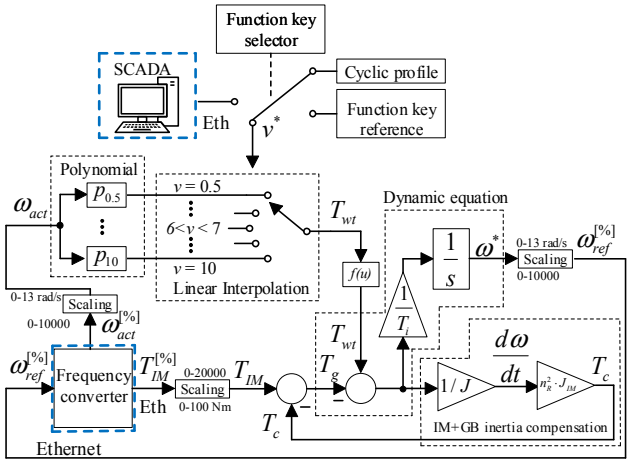

Fig. 5. The arhitecture of the implemented software in the intelligent relay

According to the wind speed, a selection is made between which characteristics are to be used for the interpolation. The block $f(u)$ is necessary when the mechanical components are not correctly aligned. The friction torque given by the non-alignment can be determined experimentally and added to the wind turbine torque or decrease from the PMSG torque.

The dynamic equation was implemented using equation (16) with the observation that the inertia J was introduced in the integration time constant. It is not possible to divide the difference torque by inertia before the integrator, because at low values the result will be unprecise while working with integers. Also dividing after integrator is not a solution because the maxim value of the integrator of the chosen intelligent relay is 1000, which will give a calculated reference speed of 7.06 rad/s and is insufficient for the wind turbine. The constant time T_i of the integrator is calculated using the next equation:

$$T_i = (\omega_0 \cdot J) / A_Q \tag{23}$$

where ω_0 is the maxim angular speed and A_Q is the output of the integrator.

Considering that the maxim angular speed of the IM is 730 rpm and the GB coefficient n_{GB} is 6.03, the maxim angular speed ω_0 was set to 13 rad/s. This value covers the maxim power point off all wind turbine characteristic so higher values can be neglected. The reference wind speed v can be set from a SCADA system and from the intelligent relay using functional keys. Additionally, a cyclic profile can be set, which can be also configured with the functional keys.

TABLE I. PARAMETERS OF THE WIND TURBINE

Parameters		*Value*	*Unit*
Rated power P_N		5	*kW*
Rated wind speed v_0		10	*m/s*
Inertia J_{wt}		140	*kg/m²*
Rated speed n_N		126	*rpm*
Blade swept area A		19.6	*m²*
Radius of the blade R		2.5	*m*
Maximum power coefficient C_p		0.426	
Specific density air ρ at 15 °C		1.225	*kg · m³*
Constant coefficients	C_{T0}	0.0986	
	a	0.0113	
	b	0.0222	
Nominal TSR λ		3	

TABLE II. PARAMETERS OF THE PMSG

Parameters	*Value*	*Unit*
Rated power S_N	5	kVA
Line voltage V_L	400	V
Rated current I_N	12	A
Rated speed n_N	120	rpm
Pole pairs p_1	16	
PM flux Ψ_{PM}	1.32	Wb
Synchronous inductance L_s	0.045	H
Stator resistance R_s	1.1	Ω
Core loss coefficient k_{pFe}	3.3	$kg \cdot m^2 / s$
Inertia J_g	1.05	kg/m^2

TABLE III. POLYNOMIAL COEFFICIENTS

Wind speed [m/s]	Coefficients			
	a	*b*	*c*	*d*
0.5	-2.2327	-2.7956	3.9874	0.1607
1	-1.5788	-1.9768	7.6105	0.6631
2	-0.5590	-2.7942	15.9581	2.5489
3	-0.4072	-2.5593	23.5429	5.8581
4	-0.2918	-2.6791	31.6608	10.2805
5	-0.2352	-2.6643	39.5654	16.0159
6	-0.1938	-2.6931	47.5693	22.9753
7	-0.1650	-2.7173	55.6449	31.0968
8	-0.1461	-2.6866	63.4598	40.6866
9	-0.1290	-2.7054	71.5043	51.3390
10	-0.1171	-2.6806	79.2964	63.5171

IV. SIMULATION AND EXPERIMENTAL RESULTS

The proposed WTE implementation was validated on an experimental platform as depicted in Fig. 1 and Fig. 12. The frequency converter which drives the IM is an ABB DTC inverter (ACS 800). The grid inverter is an ABB PVI-4.2-OUTD-W and the DB is a wind interface ABB 7200, both specifically designed for wind application. The PMSG has the parameters given in TABLE II. and is identical to the PMSG implemented on the existing wind turbine. The intelligent relay is a LOGO! Logic Module from Siemens with integrated PROFINET interface. The communication between the ABB inverter, relay and the SCADA is implemented through ethernet network using Modbus TCP/IP protocol.

Also, in order to validate the experimental results, simulations of the entire system were done based on the block diagram from Fig. 6, and the equations (1) - (17) described in section II. The digital simulation was performed in Matlab/Simulink. The load current I_{load} was calculated from the load curve presented in Fig. 3. The load curve was introduced as an approximated four-degree polynomial.

In order to compare the experimental and simulation results, the data from intelligent relay was acquired directly in Maltlab/Simulink using an OPC Server (KEPServer EX 6). Fig. 9 shows the computed torque characteristics by the intelligent relay versus the theoretical calculation. The discretization of the characteristic can be observed due to the sampling rate of the OPC Server. An interpolated characteristic is also plotted for v = 7.7 m/s.

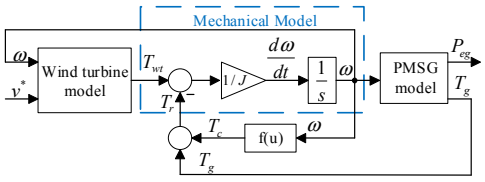

Fig. 6. Simulation block digram of the WTE

The experimental results versus simulation results are presented in Fig. 7 and Fig. 10 for a cyclic wind speed profile and in Fig. 8 and Fig. 11 for a variable wind speed profile. The measured data are the wind speed, the angular speed of the wind turbine, the wind turbine torque, PMSG torque and the electrical power provided by PMSG in the DC circuit between the DB and the inverter grid.

A digital oscilloscope, placed in the DC circuit between DB and grid inverter, is used for measuring the electric power produced by the PMSG.

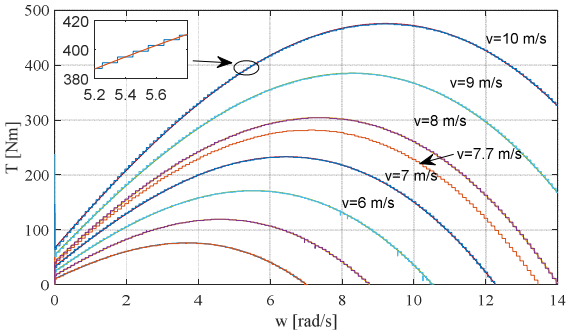

Fig. 9. The torque characteristic computed by the intelligent relay versus theoretical characteristic

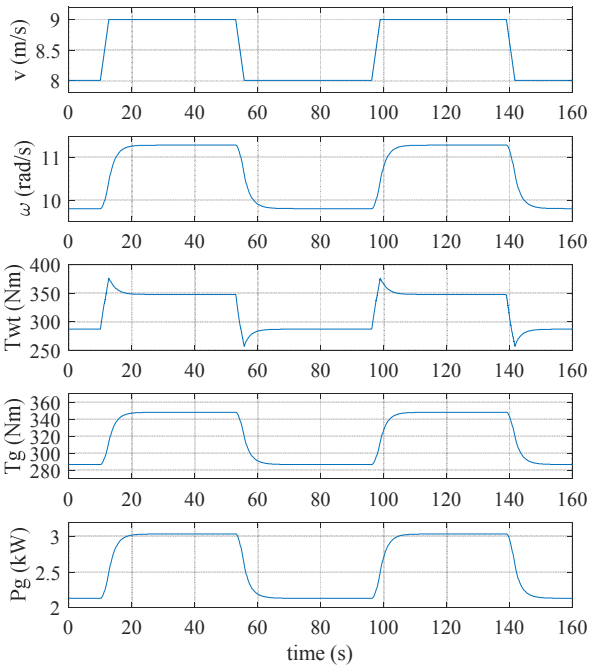

Fig. 7. Simulation results for wind speed between 8 and 9 m/s

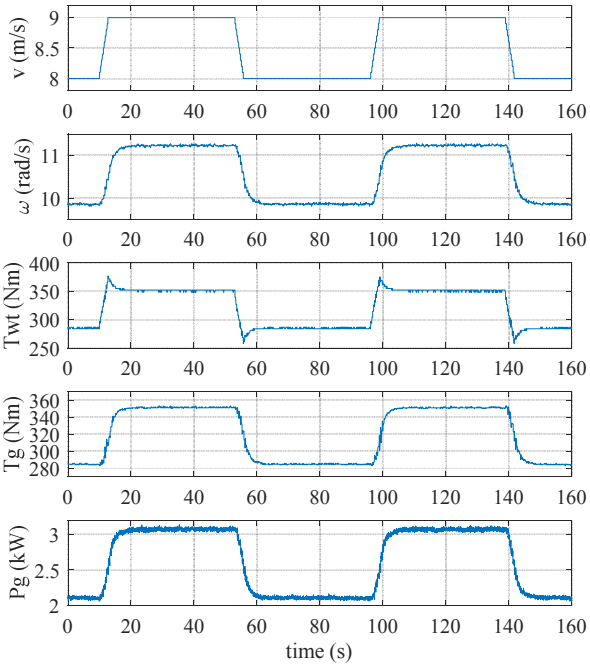

Fig. 10. Experimental results for wind speed between 8 and 9 m/s

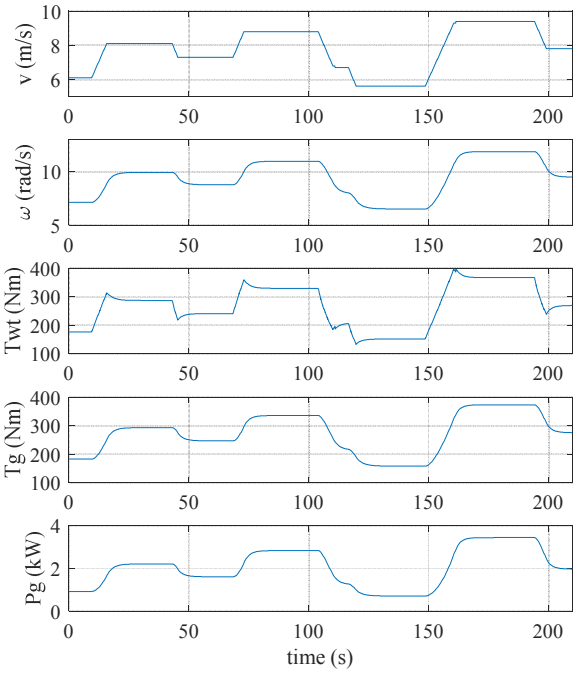

Fig. 8. Simulation results for a variable wind speed profile

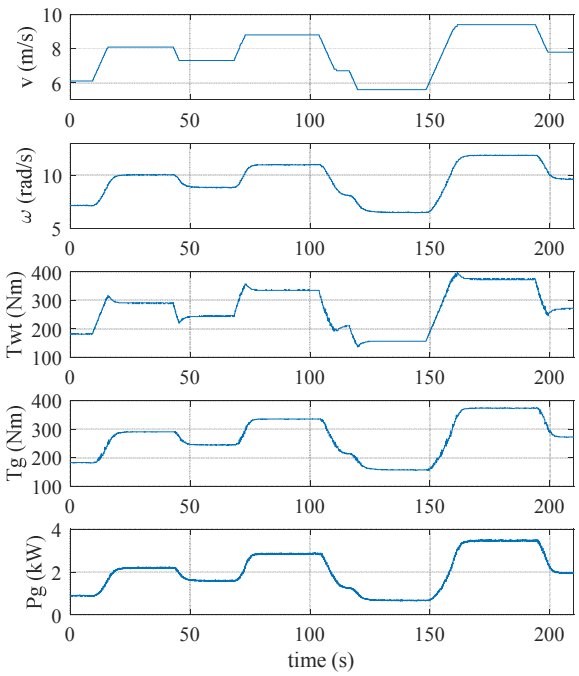

Fig. 11. Experimental results for a variable wind speed profile

Fig. 12. Experimental platform - left, The existing wind turbine - right

V. Conclusions

A hardware-in-the-loop wind turbine emulator was proposed, built with industrial equipment, including a low-cost intelligent relay which implements the wind turbine dynamic model. The advantages of this setup are also ease of use and implementation, sensorless torque and speed estimation, easy integration to other industrial systems (SCADA), and high reliability. The simulation and experimental results (performed for a low power, 5kW wind turbine system), in good correspondence, validate the theoretical considerations and the technical solutions used for this purpose.

The possibility of using the emulator for educational purposes is also considered, because of the high reliability of the industrial equipment and quick startup.

Acknowledgment

This work was supported by a grant of the Romanian Ministry of Research and Innovation, CCCDI – UEFISCDI, project number PN-III-P1-1.2-PCCDI-2017- 0391 / CIA_CLIM – *"Smart buildings adaptable to the climate change effects"*, within PNCDI III.

This work was also supported by a grant of the Romanian Ministry of Research and Innovation no. 10PFE/16.10.2018, PERFORM-TECH-UPT - The increasing of the institutional performance of the Polytechnic University of Timişoara by strengthening the research, development and technological transfer capacity in the field of "Energy, Environment and Climate Change".

References

[1] X. Wu, H. Li, X. Wang, and W. Zhao, "Cooperative Operation for Wind Turbines and Hydrogen Fueling Stations with on-site Hydrogen Production," *IEEE Transactions on Sustainable Energy*, pp. 1–1, 2020, doi: 10.1109/TSTE.2020.2975609.

[2] M. Hemmati, B. Mohammadi-Ivatloo, M. Abapour, and A. Anvari-Moghaddam, "Optimal Chance-Constrained Scheduling of Reconfigurable Microgrids Considering Islanding Operation Constraints," IEEE *Systems Journal*, pp. 1–10, 2020, doi: 10.1109/JSYST.2020.2964637.

[3] F. Chishti, S. Murshid, and B. Singh, "Robust Normalized Mixed-Norm Adaptive Control Scheme for PQ Improvement at PCC of a Remotely Located Wind–Solar PV-BES Microgrid," *IEEE Transactions on Industrial Informatics*, vol. 16, no. 3, pp. 1708–1721, Mar. 2020, doi: 10.1109/TII.2019.2923641.

[4] A. Parizad and Konstadinos. J. Hatziadoniu, "Multi-Objective Optimization of PV/Wind/ESS Hybrid Microgrid System Considering Reliability and Cost Indices," in *2019 North American Power Symposium (NAPS)*, Oct. 2019, pp. 1–6, doi: 10.1109/NAPS46351.2019.9000396.

[5] Z. Dekali, L. Baghli, and A. Boumediene, "Experimental Emulation of a Small Wind Turbine Under Operating Modes Using DC Motor," in *2019 4th International Conference on Power Electronics and their Applications (ICPEA)*, Sep. 2019, pp. 1–5, doi: 10.1109/ICPEA1.2019.8911194.

[6] I. E. Damian, M. Iacchetti, and J. Apsley, "Emulation of prime movers in wind turbine and diesel generator systems for laboratory use," in *2019 21st European Conference on Power Electronics and Applications (EPE '19 ECCE Europe)*, Sep. 2019, p. P.1-P.10, doi: 10.23919/EPE.2019.8914799.

[7] C. Vlad *et al.*, "Wind Turbine Emulation Using Permanent Magnet Synchronous Generator," in *2018 22nd International Conference on System Theory, Control and Computing (ICSTCC)*, Oct. 2018, pp. 46–52, doi: 10.1109/ICSTCC.2018.8540664.

[8] N. Muntean, L. Tutelea, D. Petrila, and O. Pelan, "Hardware in the loop wind turbine emulator," in *International Aegean Conference on Electrical Machines and Power Electronics and Electromotion, Joint Conference*, Sep. 2011, pp. 53–58, doi: 10.1109/ACEMP.2011.6490568.

[9] A. Merabet, K. A. Tawfique, Md. A. Islam, S. Enebeli, and R. Beguenane, "Wind turbine emulator using OPAL-RT real-time HIL/RCP laboratory," in *2014 26th International Conference on Microelectronics (ICM)*, Dec. 2014, pp. 192–195, doi: 10.1109/ICM.2014.7071839.

[10] Y. Sirouni, S. E. Hani, N. Naseri, A. Aghmadi, and K. E. Harouri, "Design and Control of a Small Scale Wind Turbine Emulator with a DC Motor," in *2018 6th International Renewable and Sustainable Energy Conference (IRSEC)*, Dec. 2018, pp. 1–6, doi: 10.1109/IRSEC.2018.8702899.

[11] J. J. G. Rojas, D. A. Z. Prada, and W. A. L. M. O. Lopez-Santos, "Real-Time Small-Scale Wind Turbine Emulator for a Hybrid Microgrid Laboratory Testbed," in *2019 IEEE Workshop on Power Electronics and Power Quality Applications (PEPQA)*, May 2019, pp. 1–6, doi: 10.1109/PEPQA.2019.8851573.

[12] E. Mohammadi, R. Fadaeinedjad, and H. R. Naji, "Platform for design, simulation, and experimental evaluation of small wind turbines," *IET Renewable Power Generation*, vol. 13, no. 9, pp. 1576–1586, 2019, doi: 10.1049/iet-rpg.2018.5507.

[13] J. Andrzej and B. Janusz, "Laboratory setup with squirrel-cage motors for wind turbine emulation," in *2018 Applications of Electromagnetics in Modern Techniques and Medicine (PTZE)*, Sep. 2018, pp. 1–4, doi: 10.1109/PTZE.2018.8503145.

[14] I. Moussa, A. Bouallegue, and A. Khedher, "New wind turbine emulator based on DC machine: hardware implementation using FPGA board for an open-loop operation," *IET Circuits, Devices Systems*, vol. 13, no. 6, pp. 896–902, 2019, doi: 10.1049/iet-cds.2018.5530.

[15] M. Vardia, P. C. Bapna, V. K. Yadav, and K. G. Sharma, "Performance Analysis of 1.2 kW Laboratory Prototype of MC interfaced Wind Turbine Emulator," in *2018 IEEE Industry Applications Society Annual Meeting (IAS)*, Sep. 2018, pp. 1–7, doi: 10.1109/IAS.2018.8544495.

[16] A. Ramanath, J. D. Manian Deivanayagam, S. Raju, and N. Mohan, "An Extremely Low-Cost Wind Emulator," in *IECON 2018 - 44th Annual Conference of the IEEE Industrial Electronics Society*, Oct. 2018, pp. 1675–1680, doi: 10.1109/IECON.2018.8592727.

[17] Vo Thanh Ha, Vu Hoang Phuong, Nguyen Tung Lam, and Nguyen Phung Quang, "A dead-beat current controller based wind turbine emulator," in *2017 International Conference on System Science and Engineering (ICSSE)*, Jul. 2017, pp. 169–174, doi: 10.1109/ICSSE.2017.8030859.

[18] J. Yan, Y. Feng, and J. Dong, "Study on dynamic characteristic of wind turbine emulator based on PMSM," *Renewable Energy*, vol. 97, pp. 731–736, Nov. 2016, doi: 10.1016/j.renene.2016.06.034.

[19] J. C. F. Soltoski, P. T. P. dos Santos, and C. H. I. Font, "Development of a small scale wind turbine emulator work bench," in *2016 12th IEEE International Conference on Industry Applications (INDUSCON)*, Nov. 2016, pp. 1–8, doi: 10.1109/INDUSCON.2016.7874577.

[20] M. Fatu, C. Lascu, G.-D. Andreescu, R. Teodorescu, F. Blaabjerg, and I. Boldea, "Voltage Sags Ride-Through of Motion Sensorless Controlled PMSG for Wind Turbines," in *2007 IEEE Industry Applications Annual Meeting*, Sep. 2007, pp. 171–178, doi: 10.1109/07IAS.2007.74.